

Evaluation of Pulse Contour Markers using an A-Mode Ultrasound: Association with Carotid Stiffness Markers and Ageing

Rahul Manoj, Raj Kiran V, Nabeel P M, *Member IEEE*, Mohanasankar Sivaprakasam and Jayaraj Joseph

Abstract— Vascular ageing is directly associated with the blood vessel wall structural and functional abnormalities. Pulse morphology carries information on these abnormalities, and pulse contour analysis (PCA) identifies key amplitudes and timing information on the pulse waveforms that has a prognostic value towards cardiovascular risk stratification. PCA markers derived from second derivative waveforms represent the accelerative and decelerative phase of an arterial pulse. In this work, second derivative diameter waveforms of central arteries such as carotid artery are obtained using an A-mode ultrasound device. The derived PCA markers (b/a, c/a, d/a, e/a, (b-c-d-e)/a) from diameter waveform is investigated for its association with central stiffness markers and aging. An observational and cross-sectional study on 106 subjects (51 male/55 females) was conducted for this investigation. The highest correlation ($r = 0.5$, $p < 0.001$) was observed between c/a and PWV, and the lowest correlation was between e/a and AC. Group average values of PCA markers for each age decade group were correlated strongly ($r > 0.9$, $p < 0.001$) with age. A change $> 19\%$ was observed between the group average values of PCA markers of the normotensive and hypertensive population. The applicability of aforesaid PCA markers on central pulse waveforms, measured using a noninvasive device in resource-limited field settings, would accelerate such large scale vascular screening that is essential to understanding the cardiovascular risks at a population level.

Clinical Relevance— This study provides an investigation into using second derivative diameter waveforms obtained from the carotid artery to find its associations with arterial stiffness and ageing.

I. INTRODUCTION

Vascular ageing is associated with impairments in structural and functional properties of the arterial wall. Age-related changes in the arteries will include luminal dilation, increase in stiffness, endothelial dysfunction and an increase in wall thickness [1]. Arterial stiffness is caused due to accelerated fragmentation and depletion of elastin and deposition of collagen in the media layer (increasing the intima-media thickness) [2]. The stiffening of the vessel walls causes the augmentation in the central blood pressure and early

return of the reflection waves [3]. Age-associated changes are accelerated in the presence of cardiovascular diseases, causing early vascular ageing.

Alterations in arterial pulse waveform (pressure, diameter, flow velocity) morphology is a direct consequence of the abnormalities in the vessel wall. Pulse contour analysis (PCA) is a method that identifies fiducial points (both amplitude and timing information), and derived parameters are potential markers for stiffness estimation and cardiovascular risk stratification. The PCA markers derived from second derivative pulse waveforms includes b/a, c/a, d/a, e/a and (b-c-d-e)/a, where a, b, c, d, e are amplitudes of local maxima or minima on the second derivative waveform. However, all the markers vary substantially with the vessel wall stiffness. Markers b/a and c/a carry information pertaining to the systolic phase, whereas d/a and e/a convey information in the diastolic phase. The marker (b-c-d-e)/a (sometimes referred to as Vascular Aging Index) is a cumulative effect of all the markers. The second derivative-based PCA is commonly performed on digital or peripheral pulse signals and is used as surrogate for estimating central arterial stiffness [4]. Most of the conventions in defining these markers are referred to elsewhere [5]. The usability of pressure, diameter or volume signals for deriving PCA markers are comparable in nature [6].

The applicability of aforesaid PCA markers on central pulse waveforms, measured using a noninvasive device in a resource-limited field setting, would accelerate such large scale vascular screening that is essential to understanding the cardiovascular risks at a population level. In this context, noninvasive assessed diameter waveforms of central arteries such as the carotid artery, using inexpensive, image-free ultrasound-based systems make such assessments practically possible.

In this work, we are i) evaluating PCA markers derived from the carotid diameter waveform using an image-free A mode ultrasound device and ii) investigating the association of the derived PCA markers with clinically relevant central stiffness markers and ageing. The following subsections describe the details of the device study protocol in detail, followed by significant observations and allied future works.

II. MATERIALS AND METHODS

A. A-Mode Ultrasound Device

The device consists of i) custom-made single-channel ultrasound transducer (center frequency: 10 MHz, diameter: 5 mm, spatial angle $< 1.3^\circ$, axial resolution: 140 μm) enclosed in an ergonomically designed 3D printed probe, ii) data acquisition and control hardware, iii) power supply unit and iv) Graphical User Interface (GUI) in a Windows[®] 10 running

Rahul Manoj and Raj Kiran V are with the Electrical Engineering Department, Indian Institute of Technology Madras, Chennai-600036, India (e-mail: rahulmanojktym@gmail.com).

Nabeel P M is with Healthcare Technology Innovation Centre (HTIC), Indian Institute of Technology Madras Research Park, Chennai-600113, India.

Jayaraj Joseph is with the faculty of Electrical Engineering Department. Mohanasankar Sivaprakasam is the Director of Healthcare Technology Innovation Centre and with the faculty of Electrical Engineering Department at Indian Institute of Technology Madras, Chennai-600036, India

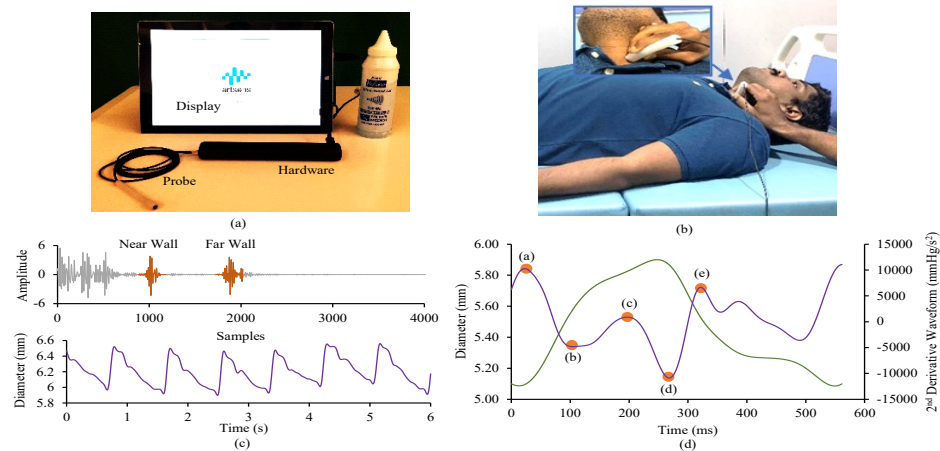


Fig.1(a) Device hardware and ultrasound probe, (b) probe positioning at carotid artery on a supine subject, (c) RF echoes from near and far wall of carotid artery with processed diameter waveform, (d) an illustration of second derivative PCA markers

tablet. This device is the most evolved form of our extensively validated ARTSENS[®] technology [7]–[10]. Fig.1(a) illustrates the hardware overview of the device.

The ultrasound transducer is isonated with a high voltage pulse train of $\pm 40V$ (frequency: 10MHz), using a pulser unit (STHV748, STMicroelectronics) in pulse-echo mode. The necessary digital controls to STHV748 to switch between transmit/receive modes are driven by the microprocessor (LPC4370FET256, 32-bit ARM Cortex, NXP Semiconductors). The radiofrequency (RF) echoes are received for a scan depth of 40 mm ($\sim 52 \mu s$ of RF signals per frame) by the high-speed analog to digital converters (ADC) of the microprocessor at an 80 MHz sampling rate. The microprocessor is connected to a tablet running on Windows[®] 10 via USB 2.0 for GUI and data transfer. The pulse repetition rate or the frame rate is fixed at 40 Hz.

B. Study Population and Protocol

An in-vivo study, consisting of 51 male and 55 female participants ($n = 106$), was conducted in a multi-speciality hospital, Chennai, India. The study protocols were reviewed and approved by the Institutional Review Board (VHS-IEC/17-2016). A written consent acknowledging their participation, in accordance with the World Medical Association Declaration of Helsinki: Ethical principles for medical research involving human subjects, revised in 2013, was provided by the participants. Anthropometric measurements, including height, weight, and body mass index (BMI), were collected prior to the measurement. The participants were made fully aware of the objectives of the study. The participants were allowed to rest for 5 mins in the supine posture, followed by brachial BP measurements on the left arm. The left common carotid artery was identified by palpation for performing an image-free ultrasound measurement, and the ultrasound probe was positioned and oriented on the subject's neck in the supine position. The probe needs to be aligned normal to the pulsating artery walls so that the echoes are sharp (higher signal quality). The narrow half-angle beam width and poor off-axis sensitivity ensure measurements are performed along the true diameter of the artery. Two trials were recorded for each participant. Fig.1(b) demonstrates the probe positing at the carotid artery on the subject.

C. Data Processing

The RF echoes are continuously tracked for near-wall and far-fall of the carotid artery and are converted to a diameter waveform (Fig.1(c)). The algorithm that performs the RF echoes to diameter conversion has been extensively validated. The digitized RF echoes are processed on a LabVIEW[®] based application. A 4th order bandpass zero-phase filter with low cut off: 1 MHz and high cut off: 8 MHz was used to process the RF echoes. The obtained diameter waveform is scaled to carotid pressure waveform using an empirically derived exponential relationship between pressure and arterial cross-sectional area [11] and then calibrated using brachial mean arterial pressure and diastolic BP. Thus, obtained carotid pressure waveform along with the diameter waveform is used to evaluate the central stiffness parameters. The diameter waveforms were filtered using a Savitzky–Golay's filter of 3rd order polynomial and 15 side points, ensuring a 3dB cut-off in the frequency spectrum of derivatives to be at 12 Hz. The fiducial points (a, b, c, d, e) are identified as illustrated in Fig.1(d) for evaluating the PCA markers.

D. Statistical Analysis

All continuous variables are presented as mean \pm standard deviations. Independent and multi-variate regression analyses were performed between PCA markers, stiffness markers and age. The correlation was reported in terms of Pearson's correlation coefficient (r) and statistical significance in the p -value. Box-and-whisker plots were the ranges of PCA markers across the hypertensive and normotensive population. The level of significance of $\alpha = 0.05$ was used for all tests. A p -value > 0.05 confirmed a statistical significance.

III. RESULTS AND DISCUSSIONS

A. Subject Demography

The study population consists of 106 participants (51 male and 55 female) aged 42 ± 15 years. The average systolic blood pressure (SBP) was 128.94 ± 22.16 mmHg, and the average diastolic blood pressure (DBP) was 79.97 ± 13.01 mmHg. Five subjects had a history of smoking, and four subjects had an active lifestyle. Six subjects had above-normal body mass index (BMI). 42 subjects were classified as hypertensive (SBP > 140 mmHg and DBP > 90 mmHg), and 64 as

TABLE I SUBJECT DEMOGRAPHY

Total Subjects	106
Male	51
Female	55
Age	18 – 71
Normotensive subjects	64
Hypertensive subjects	42
Systolic blood pressure (mmHg)	90 – 208
Diastolic blood pressure (mmHg)	50 – 107
β	1.51 – 15.20
Elastic modulus (kPa)	19.48 – 255.47
PWV (m/s)	3.03 – 10.97
Arterial Compliance (mm ² /kPa)	0.28 – 2.52

normotensive (SBP: 90 – 140 mmHg, DBP: 60 – 100 mmHg). A summary of the subject demography is presented in TABLE I.

B. Reliability of Signals

The RF echoes had an SNR > 20 dB. The high-fidelity RF echoes were tracked with a spatial resolution of 10 μ m. The obtained diameter waveforms were quasi-periodic and continuous in nature, with a temporal resolution of 4 ms. The group average end-diastolic diameter (D_d) and distension (ΔD) were 5.99 ± 1.44 mm and 0.43 ± 0.14 mm. The group average values of PCA markers b/a , c/a , d/a , e/a and $(b-c-d-e)/a$ are -0.69 ± 0.41 , 0.07 ± 0.14 , -0.33 ± 0.22 , 0.22 ± 0.22 and -0.64 ± 0.55 respectively.

C. Association of PCA Markers with Stiffness Markers

A summary of the pair-wise regression analysis ($p < 0.001$) with each of the PCA markers (b/a , c/a , d/a , e/a and $(b-c-d-e)/a$) with each of the central stiffness markers (β , E_p , AC, PWV) is depicted in TABLE II. The highest correlation among all the set, was observed between c/a and PWV ($r = 0.50$, $p < 0.001$). The least correlation was between e/a and AC ($r = 0.16$, $p < 0.001$).

PCA markers derived from the second derivative waveforms directly measure the accelerative and decelerative phases of the arterial wall dynamics (in the case of diameter signals) [13]. As the artery gets stiffer due to ageing or due to any underlying diseases, the buffering action of the central arteries is compromised, increasing the load of the heart [14]. The aforesaid PCA markers can provide information pertaining to the dynamic changes in the arterial wall through the cycle-to-cycle changes in the amplitudes of a , b , c , d , e points of second derivative waveforms. However, the conventional stiffness markers provide an average estimate of the arterial wall dynamics. Further investigations are required to explore the variation in PCA markers with the incremental nature of PWV [15]–[17].

TABLE II PAIR-WISE REGRESSION ANALYSIS (R-VALUE)

	b/a	c/a	d/a	e/a	$(b-c-d-e)/a$
β	0.32	-0.42	0.21	-0.26	0.36
E_p	0.34	-0.46	0.23	-0.29	0.39
AC	-0.27	0.38	-0.15	0.16	-0.30
PWV	0.38	-0.50	0.24	-0.31	0.44
Age	0.46	-0.60	0.25	-0.34	0.53

D. Association of PCA Markers with Age and Hypertensive /Normotensive Classification

A statistically significant and moderate correlation was observed between c/a and age ($r = 0.60$, $p < 0.001$). The r -value of pair-wise regression analysis of each of the PCA markers with age is presented in TABLE II. Fig.2(a)-(e) depicts the age-related trend for the group average values for each PCA markers within each age bin (< 20, 20-29, 30-39, 40-49, 50-59 and > 60 (years)). The bin-wise group average b/a and $(b-c-d-e)/a$ had a positive correlation with age ($r > 0.95$, $p < 0.001$) and the other markers had a negative correlation ($r > 0.92$, $p < 0.001$). A change > 19% was observed between the group average values of PCA markers of the normotensive and hypertensive population, as depicted in Fig.2(f). The largest change from normotensive to hypertensive was observed for c/a with 74% (decrease in mean value)

The age-related trends were at par with the trends reported in previous studies [4], [18]. Vascular ageing is predominantly characterized by the stiffening of the central arteries and disappearance of the stiffness gradient (central to peripheral) [19], eventually resulting in hypertension. The association of PCA markers with ageing and hypertension has the potential to be associated with the multi-factor vascular ageing index [1], [20], which could provide a single index to characterize the ageing of the vasculature. Treatment strategies for hypertension have started to shift from the classical approach of merely looking at the reduction in the levels of SBP and DBP to include a reduction in stiffness markers, wave reflection and pulse pressure [21]. The confounding effect of heart rate, respiratory rate, and ECG are not investigated in this current study. The advent of wearable platforms enables continuous monitoring of ECG [22], [23], heart rate [24], respiratory rate [25], [26], when combined with conventional markers, would provide further insights into the dynamics of PCA markers. The scope of PCA is not just limited to second derivative waveforms-based markers, and the inclusions of such derived markers to a vascular ageing index and hypertensive treatment strategies need to be explored.

IV. CONCLUSION

This work has demonstrated the applicability of the second derivative based PCA markers on a central pulse waveform such as carotid artery diameter using an A-mode ultrasound device. Further, the association of PCA markers with central stiffness markers (β , E_p , AC, PWV) was analyzed and had a moderate correlation between them. The group average

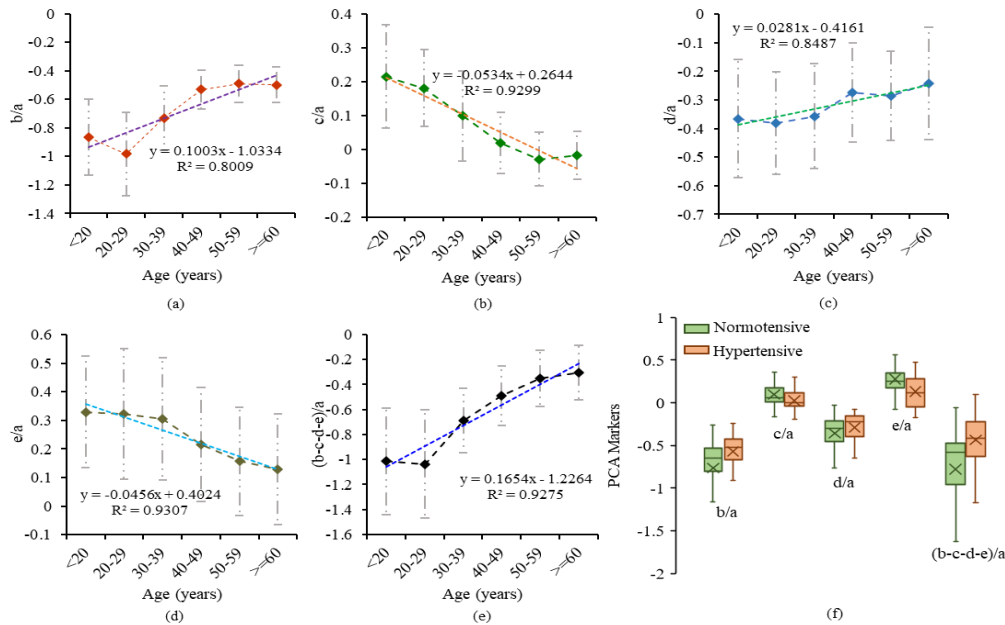


Fig.2. (a)-(e) Correlation plot for PCA markers with age bins, (f) the hypertensive and normotensive group classification based on the PCA markers

values for each age decade correlated strongly with age. PCA markers differed in magnitude for the hypertensive and normotensive subjects, as indicated by the percentage change in the group average values. Further investigations are suggested to include PCA markers as part of vascular index matrix calculations, not limiting to the stiffness markers.

REFERENCES

- [1] S. Laurent, "Defining vascular aging and cardiovascular risk," *J. Hypertens.*, vol. 30, no. SUPPL. 1, pp. 3–8, 2012.
- [2] S. Laurent et al., "Structural and genetic bases of arterial stiffness," *hypertension*, vol. 45, no. 6, pp. 1050–1055, Jun. 2005.
- [3] W. W. Nichols, "Clinical measurement of arterial stiffness obtained from noninvasive pressure waveforms," *Am. J. Hypertens.*, vol. 18, no. 1 SUPPL., pp. 3–10, Jan. 2005.
- [4] D. M. Gvozdić et al., "Novel mechanism for order-of-magnitude enhancement of rashba effect in wide modulation-doped quantum wells," in *AIP Conference Proceedings*, 2007, vol. 893, pp. 1371–1372.
- [5] E. Von Wowern et al., "Digital photoplethysmography for assessment of arterial stiffness: Repeatability and comparison with applanation tonometry," *PLoS One*, vol. 10, no. 8, pp. 1–19, 2015.
- [6] M. Elgendi, "Standard Terminologies for Photoplethysmogram Signals," *Curr. Cardiol. Rev.*, vol. 8, no. 3, pp. 215–219, 2012.
- [7] J. Joseph et al., "Assessment of Carotid Arterial Stiffness in Community Settings with ARTSENS®," *IEEE J. Transl. Eng. Heal. Med.*, vol. 9, no. November 2020, 2021.
- [8] J. Joseph et al., "ARTSENS® Pen - Portable easy-to-use device for carotid stiffness measurement: Technology validation and clinical-utility assessment," *Biomed. Phys. Eng. Express*, vol. 7, no. 2, 2020.
- [9] A. K. Sahani et al., "Automatic measurement of end-diastolic arterial lumen diameter in ARTSENS," *J. Med. Devices, Trans. ASME*, vol. 9, no. 4, p. 041002, 2015.
- [10] A. K. Sahani, et al. "Automated system for imageless evaluation of arterial compliance," *Proc. Annu. Int. Conf. IEEE Eng. Med. Biol. Soc. EMBS*, pp. 227–231, 2012.
- [11] J. M. Meinders et al., "Simultaneous assessment of diameter and pressure waveforms in the carotid artery," *Ultrasound Med. Biol.*, vol. 30, no. 2, pp. 147–154, 2004.
- [12] P. M. Nabeel, et al. "Local Pulse Wave Velocity: Theory, Methods, Advancements, and Clinical Applications," *IEEE Rev. Biomed. Eng.*, vol. 13, no. c, pp. 74–112, 2020.

- [13] Y. J. Park et al., "Association of the second derivative of photoplethysmogram with age, hemodynamic, autonomic, adiposity, and emotional factors," *Med. (United States)*, vol. 98, no. 47, 2019.
- [14] C. Giannattasio, "Arterial stiffness," *Curr. Hypertens. Rep.*, vol. 6, no. 5, pp. 331–332, 2004.
- [15] P. M. Nabeel et al., "A Magnetic Plethysmograph Probe for Local Pulse Wave Velocity Measurement," *IEEE Trans. Biomed. Circuits Syst.*, vol. 11, no. 5, pp. 1065–1076, 2017.
- [16] P. M. Nabeel et al., "Variation in local pulse wave velocity over the cardiac cycle: in-vivo validation using dual-MPG arterial compliance probe," *13th Russ. Conf. Biomed. Eng.*, pp. 100–103, 2018.
- [17] P. M. Nabeel et al., "Bi-Modal arterial compliance probe for calibration-free cuffless blood pressure estimation," *IEEE Trans. Biomed. Eng.*, vol. 65, no. 11, pp. 2392–2404, 2018.
- [18] K. Takazawa et al., "Assessment of vasoactive agents and vascular aging by the second derivative of photoplethysmogram waveform," *hypertension*, vol. 32, no. 2, pp. 365–370, 1998.
- [19] G. M. London et al., "Arterial stiffness gradient, systemic reflection coefficient, and pulsatile pressure wave transmission in essential hypertension," *hypertension*, vol. 74, no. 6, pp. 1366–1372, 2019.
- [20] V. M. Barodka et al., "Implications of vascular aging," *Anesth. Analg.*, vol. 112, no. 5, pp. 1048–1060, May 2011.
- [21] M. E. Safar, "Arterial stiffness as a risk factor for clinical hypertension," *Nat. Rev. Cardiol.*, vol. 15, no. 2, pp. 97–105, 2018.
- [22] S. P. Preejith et al., "Wearable ECG platform for continuous cardiac monitoring," *Annu. Int. Conf. IEEE Eng. Med. Biol. Soc. IEEE Eng. Med. Biol. Soc. Annu. Int. Conf.*, vol. 2016, pp. 623–626, Oct. 2016.
- [23] B. Murugesan et al., "ECGNet: Deep Network for Arrhythmia Classification," in *MeMeA 2018 - 2018 IEEE International Symposium on Medical Measurements and Applications, Proceedings*, 2018.
- [24] S. P. Preejith et al., "Design, development and clinical validation of a wrist-based optical heart rate monitor," *2016 IEEE Int. Symp. Med. Meas. Appl. MeMeA 2016 - Proc.*, Aug. 2016.
- [25] V. Ravichandran et al., "RespNet: A deep learning model for extraction of respiration from photoplethysmogram," in *Proceedings of the Annual International Conference of the IEEE Engineering in Medicine and Biology Society, EMBS*, 2019, pp. 5556–5559.
- [26] S. P. Preejith et al., "Accelerometer based system for continuous respiratory rate monitoring," *2017 IEEE Int. Symp. Med. Meas. Appl. MeMeA 2017 - Proc.*, pp. 171–176, Jul. 2017.